Colossal magnetoresistance observed in Monte Carlo simulations of the one- and two-orbital models for manganites

Cengiz Şen,[1] Gonzalo Alvarez,[2] Horacio Aliaga,[3,4] and Elbio Dagotto[3,4]
[1]*National High Magnetic Field Laboratory and Department of Physics, Florida State University, Tallahassee, Florida 32310, USA*
[2]*Computer Science & Mathematics Division, Oak Ridge National Laboratory, Oak Ridge, Tennessee 37831, USA*
[3]*Condensed Matter Sciences Division, Oak Ridge National Laboratory, Oak Ridge, Tennessee 32831, USA*
[4]*Department of Physics and Astronomy, The University of Tennessee, Knoxville, Tennessee 37996, USA*
(Received 8 March 2006; revised manuscript received 24 April 2006; published 29 June 2006)

The one- and two-orbital double-exchange models for manganites are studied using Monte Carlo computational techniques in the presence of a robust electron-phonon coupling (but neglecting the antiferromagnetic exchange J_{AF} between the localized spins). The focus in this effort is on the analysis of charge transport. Our results for the one-orbital case confirm and extend previous recent investigations that showed the presence of robust peaks in the resistivity versus temperature curves for this model. Quenched disorder substantially enhances the magnitude of the effect, while magnetic fields drastically reduce the resistivity. A simple picture for the origin of these results is presented. It is also shown that even for the case of just one electron, the resistance curves present metallic and insulating regions by varying the temperature, as it occurs at finite electronic density. Moreover, in the present study these investigations are extended to the more realistic two-orbital model for manganites. The transport results for this model show large peaks in the resistivity versus temperature curves, located at approximately the Curie temperature, and with associated large magnetoresistance factors. Overall, the magnitude and shape of the effects discussed here resemble experiments for materials such as $La_{0.70}Ca_{0.30}MnO_3$, and they are in agreement with the current predominant theoretical view that competition between a metal and an insulator, enhanced by quenched disorder, is crucial to understanding the colossal magnetoresistance (CMR) phenomenon. However, it is argued that further work is still needed to fully grasp the experimentally observed CMR effect, since in several other Mn oxides an antiferromagnetic charge-ordered orbital-ordered state is the actual competitor of the ferromagnetic metal.

DOI: 10.1103/PhysRevB.73.224441 PACS number(s): 75.47.Lx, 75.30.Mb, 75.30.Kz

I. INTRODUCTION

One of the most outstanding open problems in the area of transition metal oxides is the explanation of the colossal magnetoresistance (CMR) effect that appears in the Mn oxides that are widely referred to as manganites. These compounds present a rich phase diagram with a variety of competing states which are stabilized by changing the carrier concentration using a standard chemical doping process involving ions with different valences, or by varying the carrier bandwidth via isovalent doping.[1–29] Notorious among the low-temperature regimes stabilized in manganites are a ferromagnetic (FM) metallic phase and several antiferromagnetic/charge/orbital ordered insulating states. For the compounds with intermediate or small Curie temperatures, the experimentally obtained resistivity versus temperature curves present a sharp peak, which occurs precisely at the transition toward ferromagnetism. In the vicinity of this peak, the CMR effect is observed, which consists of enormous changes in the resistivity upon the introduction of relatively small magnetic fields. Although technological applications of CMR compounds in the read-sensor industry will still need an increase by at least a factor 2 of the currently available critical temperatures where the large magnetoeffects occur, the physics behind this remarkable CMR phenomenon defines a challenging basic-science problem that has attracted the attention of the condensed matter community.

The explanation of the CMR effect is certainly the crucial goal of theoretical investigations in the manganite context. Early theoretical work showed that the standard double exchange (DE) model was not sufficient to understand these materials.[17] In fact, a DE model cannot even produce an insulator at high temperatures, in the realistic regimes of electronic densities,[30] and this pointed toward the importance of other couplings, such as electron-phonon, for a proper description of these compounds.[18] Progress was later made with the realization that manganite models have tendencies toward mixed phase regimes, typically involving metallic and insulating states in coexistence.[4,20] This discovery was possible only after the DE model and its close variations were studied with unbiased computational methods beyond mean-field approximations. Inhomogeneous states with a variety of length scales appear frequently in these studies and the full strength of computational techniques is clearly needed to fully understand this and other families of complex oxides.[3] The theoretical discovery of phase separation tendencies[15,31,32] triggered an enormous experimental effort that confirmed the relevance of mixed states in most of the CMR compounds (for a review see Ref. 10). Percolative pictures were envisioned to understand these materials. Model calculations by Mayr *et al.*[33] and Burgy *et al.*,[34,35] using simplified spin systems and random resistor networks, revealed a phenomenology very similar to that of real CMR materials in the regime of couplings and electronic densities where metallic and insulating states were in competition. In fact, a large peak in the resistivity of the resistor network was found at intermediate temperatures, and a huge change in its value was found to occur in the presence of magnetic fields. The

key role of quenched disorder was noted in these investigations, to obtain large enough effects.[34,35]

This initial effort using simple models was followed by calculations of resistivities in the more realistic, although still simplified, one-orbital model for manganites. Verges *et al.*[21] numerically showed that an insulator can appear at intermediate and large temperatures if the electron-phonon coupling λ is robust enough. This regime, caused by localized polarons, is followed by a rapid transition to a metal upon cooling. In this model, the two tendencies in competition at low temperatures are *both* ferromagnetic, and they only differ in the character of the charge distribution (uniform versus localized). Although having two competing FM states cannot solve the entire CMR issue, since often the competition in experiments is between a ferromagnet against an antiferromagnetic/charge/orbital ordered state, the results were sufficiently interesting and challenging that they deserved further work. Moreover, they could be of relevance to important Mn oxides such as $La_{0.7}Ca_{0.3}MnO_3$, which at least naively seem well separated from charge ordered states in the phase diagrams. Recently, Kumar and Majumdar[36] made a very important contribution by proposing a new Monte Carlo (MC) algorithm to study fairly large lattices of the one-orbital model including phonons. Their main observation is that the clean limit results of Ref. 21 are much enhanced by including on-site quenched disorder, together with a robust electron-phonon coupling.[37] This role of disorder to trigger polaron formation in systems with strong electron-lattice coupling is an effect that complements the nanoscale phase coexistence near a first-order transition boundary also triggered by quenched disorder emphasized in other studies.[34,35] Large peaks in the resistivity versus temperature curves were reported in Ref. 36, resembling experiments for some manganites. Their conclusion regarding the importance of disorder was in agreement with previous investigations,[34,35,38–40] and provided further confirmation of the currently widely accepted view of manganites, namely that the essence of CMR lies in the competition of phases (metal versus insulator), supplemented by quenched disorder to obtain large enough effects in sufficiently wide regions of parameter space.

In spite of this tremendous progress, there are still several aspects of the CMR problem that need further refinement. Two issues are notable: (i) It is important to show that the results previously obtained for the one-orbital model, focusing on the resistivity peak, do also appear for a more realistic two-orbital model. Several manganites present orbital order and, as a consequence, using two orbitals per Mn atom is crucial for a proper description of these materials. (ii) The consideration of the antiferromagnetic spin coupling J_{AF} between the localized t_{2g} spins is also crucial. For instance, this coupling is needed to stabilize several important phases with charge/orbital and antiferromagnetic order, as previously shown.[10,41] The full understanding of the CMR effect needs these two extra refinements.

In the present paper, investigations of both the one- and two-orbital models for manganites are reported, with emphasis on the resistivity versus temperature curves. The main results discussed in this paper are the following: (1) We provide an independent confirmation of the results of previous investigations discussed in Refs. 21 and 36. The study of resistivity in Ref. 36 relied on the analysis of the optical conductivity extrapolated to zero frequency. In addition, a novel algorithm was used to generate the classical spin configurations. In our present effort, a different numerical method (exact diagonalization) is used and, more important, the transport properties are estimated using the Landauer formalism based on transmission coefficients. Fortunately, our study shows that the results of Kumar and Majumdar[36] reporting resistivity peaks in the one-orbital model are indeed qualitatively correct, even when a fairly different approach is used to calculate transport properties. This confirmation of previous investigations helps provide a robust foundation for computational studies of models for manganites. (2) Still within the one-orbital model context, here a comprehensive analysis of the influence of quenched disorder and electronic density is provided, thus considerably extending the studies reported in previous efforts. A surprising result is that even just one e_g electron on a finite lattice can present transmission characteristics that include a resistance versus temperature curve in qualitative agreement with results at finite electronic densities n and with experiments. Charge localization is found to be responsible for all these features, as previously remarked in Refs. 21 and 36 as well. A toy example is here discussed to understand these results in very simple terms. (3) Finally, one of our main new contributions is the extension of the previous investigations in the one-orbital model context into a two-orbital model framework. After a comprehensive analysis of the two-orbital model properties, reported here, it is concluded that this model presents a phenomenology similar to that of the one-orbital model simulations, at least for the case $J_{AF}=0$. In other words, sharp peaks in the resistivity versus temperature are observed in robust regions of parameter space. This conclusion adds more evidence that theoretical investigations are on the right track toward an understanding of the challenging CMR effect.

However, the important inclusion of J_{AF} is postponed for future investigations. Working at the special case $J_{AF}=0$ greatly simplifies the numerical analysis, particularly regarding the convergence properties: the localized spins do not have conflicting tendencies, such as ferro- and antiferro arrangements with close energies, thus they rapidly tend toward ferromagnetic ground states at low temperatures, even if the initial starting Monte Carlo configuration is random. The assumption $J_{AF}=0$ effectively reduces the global effort to merely making sure that the classical lattice displacements regulated by the electron-phonon coupling are properly converged. Important metastabilities were not found in our investigations. The considerably more subtle technical difficulties that will arise with the inclusion of J_{AF} in the model Hamiltonians are left for future considerations.

A clarification about the models used here is important. In this effort, and in fact in most of theoretical work in manganites, the starting point is the double exchange model with mobile electrons interacting with localized spins. The reason is that this model leads in a natural way to most of the phases found experimentally in the Mn oxide investigations, and in addition efforts as reported here and in related literature have also found large magnetoresistance effects. However, other

points of view have been expressed based on the pairing of oxygen holes into heavy bipolarons.[42] Clearly, the physics of manganites is sufficiently complex that several perspectives exist in the literature and further work will clarify which approach is the best to understand the CMR effect.

The organization of the paper is the following. In Sec. II, results for the one-orbital model are presented, starting with a brief discussion of the model itself and technical aspects. The main portion of this section is devoted to the numerically calculated resistivity versus temperature curves, obtained at several electronic densities, electron-phonon couplings, and strength of the quenched disorder. The results for the one electron problem are included in this section, together with evidence that charge localization is responsible for the insulating regime. A simple toy example is presented to understand the results. In Sec. III, a similar analysis is presented but using the two-orbital model. Section IV contains the conclusions of our effort, and suggestions for further work.

II. ONE-ORBITAL MODEL

A. Definition and details of simulation

The one-orbital model used in this study is given by

$$H_{1b} = -t\sum_{\langle ij\rangle,\alpha}(c^{\dagger}_{i,\alpha}c_{j,\alpha}+\text{h.c.}) - J_H\sum_{i,\alpha,\beta} c^{\dagger}_{i,\alpha}\vec{\sigma}_{\alpha,\beta}c_{i,\beta}\cdot\vec{S}_i - \lambda t\sum_{i,\gamma,\alpha}(u_{i,-\gamma}-u_{i,\gamma})c^{\dagger}_{i,\alpha}c_{i,\alpha} + t\sum_{i,\gamma}(u_{i,\gamma})^2 + \sum_{i,\alpha}(\Delta_i-\mu)n_{i,\alpha}, \quad (1)$$

where $c^{\dagger}_{i,\alpha}$ creates an electron at site i with spin α, $\sigma_{\alpha,\beta}$ are the Pauli spin matrices, $\langle ij\rangle$ indicates nearest-neighbor sites, and t is the nearest-neighbor hopping amplitude ($t=1$ also sets the energy unit). Classical localized spin $\vec{S}_i$ represents the t_{2g} degrees-of-freedom. The third term in the Hamiltonian accounts for the energy corresponding to the lattice-carrier interaction, with λ being the strength of the electron-phonon coupling. $u_{i,\gamma}$ are the distortions of the oxygen atoms surrounding a Mn ion at site i. The index γ in three dimension (3D) [two dimension (2D)] runs over three (two) directions x,y and z (x and y). The tendency toward increasing the magnitude of the lattice distortions is balanced by the fourth term in the Hamiltonian, which represents the stiffness of the Mn-O bonds. Since the study of quantum phonons in this context is not possible with currently available algorithms, the oxygen displacements are considered classical, approximation widely used in studies of manganites.[10] Δ_i represents the strength of the disorder at a given site and are chosen from a bimodal distribution of width 2Δ with mean 0. The overall electronic density n is controlled by the chemical potential μ. In the rest of the paper, spatial labels will be denoted without arrows or bold letters independently of the dimension. Also the notation $i+j$ is meant to represent the lattice site given by the vectorial sum of the vectors corresponding to i and j, respectively.

In this manuscript, the limit of an infinite Hund coupling will be considered, which is another widely used simplification known to preserve the essential physics of manganites.[10] In this limit, the spin of the e_g-electron perfectly aligns along the localized t_{2g}-spin direction, and the Hamiltonian is reduced to

$$H_{1b} = -t\sum_{\langle ij\rangle}\left\{\left[\cos\frac{\theta_i}{2}\cos\frac{\theta_j}{2}+\sin\frac{\theta_i}{2}\sin\frac{\theta_j}{2}e^{i(\phi_i-\phi_j)}\right]d^{\dagger}_i d_j + \text{h.c.}\right\} - \lambda t\sum_{i,\gamma}(u_{i,-\gamma}-u_{i,\gamma})d^{\dagger}_i d_i + t\sum_{i,\gamma}(u_{i,\gamma})^2 + \sum_i(\Delta_i-\mu)n_i, \quad (2)$$

where θ_i and ϕ_i are the spherical coordinates of the core spin at site i (assumed classical). The operators $d^{\dagger}_i$ now create an electron at site i with spin parallel to the core spin at i, and $n_i=d^{\dagger}_i d_i$. Note that for an infinite Hund coupling, the system can be shown to be particle-hole symmetric with respect to density $n=0.5$. Thus, results at densities n and $1-n$ are equivalent.

The technique used here to handle this Hamiltonian involves the standard exact diagonalization of the quadratic fermionic sector for a given spin background updated at each Monte Carlo step.[10,20] In the one-orbital study, mainly lattice sizes 8×8 and $4\times4\times4$ were used.[43] In addition, 10^4 steps were typically employed for thermalization, followed by another 10^4 for measurements. For larger lattices, such as 12×12 and $6\times6\times6$, 10^4 measurement steps were performed after 2000 steps for thermalization. Most of the simulations have started with a random configuration of spins, but simulations with a FM starting configuration have also been carried out in order to check for convergence. Furthermore, independent Monte Carlo runs corresponding to different starting random seeds for the initial random spin configuration have also been averaged wherever possible to increase the accuracy of the results.

Note that while in principle in finite clusters it is not possible to observe true singularities associated with phase transitions, in practice a very good approximation to singular behavior can be observed. This is exemplified in Fig. 1 where the spin correlations indicate a clear sharply defined different behavior between smaller and larger temperatures, with respect to a characteristic temperature that it is safe to associate with the Curie temperature.

The resistivity ρ has been calculated by taking the inverse of the mean conductivity σ, where the latter is related to the conductance G by $G=\sigma L^{d-2}$, with d being the dimension and L the linear size of the lattice. The calculation of the conductance G has been carried out following the approach extensively discussed before by Verges.[44] The use of the resistivity notation is to facilitate the interpretation of results and comparison with experiments, namely we do not claim to have observed Ohmic behavior in our small system simulations. For the purposes of our paper, whether the resistivity or resistance is used as the key observable the conclusions are the same. The units used for the resistivity in the entire manuscript are $[h/e^2]$ in 2D, and $[hL/e^2]$ in 3D. Precisely in 3D, the results presented in the figures were obtained by multiplying the resistance by the linear size L, assuming a lattice

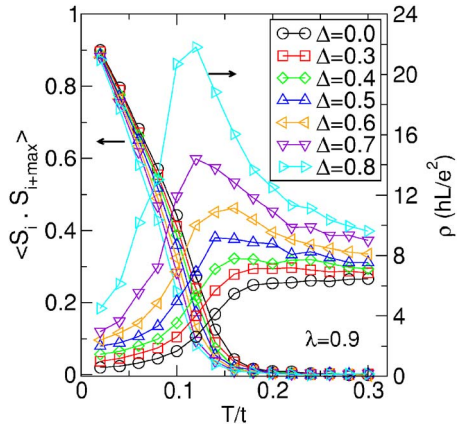

FIG. 1. (Color online) Monte Carlo results obtained using a $4\times4\times4$ lattice. Shown are the resistivity and spin-spin correlations, the latter at the maximum allowed distance ($2\sqrt{3}$), versus temperature, working at $\lambda=0.9$, $n=0.3$, and for the disorder strengths Δ indicated. The results shown are mainly for one configuration of quenched disorder, but as many as ten configurations were used in particular cases of temperatures and Δ's, and no substantial deviations were observed between disorder configurations.

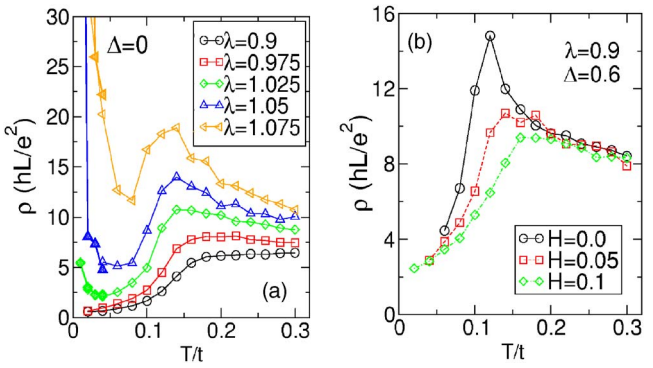

FIG. 2. (Color online) (a) Influence of the electron-phonon coupling λ in the clean limit $\Delta=0$, and (b) effect of magnetic fields (values indicated) for $\lambda=0.9$ and $\Delta=0.6$, on the resistivity curves, using a $4\times4\times4$ lattice at density $n=0.3$.

spacing one. To restore the proper units to our results, the real lattice spacing of Mn oxides must be used.

Finally, it is important to remark that a sizable portion of the computational work presented here was carried out on parallel supercomputers, in particular on the NCCS XT3 supercomputer (2.4-GHz AMD Opteron processor and 2 Gbytes of memory) at Oak Ridge National Laboratory. Typical simulations in this effort made use of 100 to 200 nodes in parallel. These supercomputer resources have decreased substantially the amount of real time that would have been needed. Indeed, we estimate that the entire effort would have taken at least one year to complete on standard small-size computer clusters. The message-passing interface was used to parallelize the runs that sweep over the various Hamiltonian parameters such as λ and temperature. Furthermore, quenched disorder adds an extra level of computational effort since it requires the simulation and average of results from many different configurations. This extra level of complexity has also been parallelized.

B. Density $n=0.3$

The discussion of our computational results starts at the electronic density $n=0.3$ (equivalent to $n=0.7$, due to the symmetry discussed in the previous section). Figure 1 is a typical example of the resistivity curves obtained in the present effort. In the clean limit, $\Delta=0$, there is a rapid change in resistivity near the transition to ferromagnetism. This is a typical pure double-exchange behavior: in the absence of a sufficiently strong λ, quenched disorder, or other couplings that may lead to competing states, then a metal is obtained at temperatures above the Curie temperature.

As already clearly established in this field, pure double-exchange models are not enough to address the physics of the CMR materials. However, note the dramatic effect of quenched disorder inducing a peak on the resistivity, as shown in Fig. 1. Even for the small systems studied here, the ratio of resistivities between its maximum and minimum values is as large as ~6 for $\Delta=0.7$. Note the correlation between the peak location and the temperature where ferromagnetic order appears (signaled in our calculations by the value of the spin-spin correlation at the largest possible distance in the cluster under investigation). The comparison of our results with those of recent publications[36] shows that the peak in the resistivity is a robust feature of the model.

Although a variety of previous theoretical and experimental investigations have convincingly shown the importance of quenched disorder in the CMR context, nevertheless it is interesting to observe that a resistivity peak can also be found by varying λ even in the clean limit $\Delta=0$, as shown in Fig. 2(a). This observation will appear repeatedly in the rest of the results discussed below, namely there seems to exist a qualitative relation between increasing Δ at small λ and simply increasing λ at $\Delta=0$. This fact will be exploited in the studies presented below to simplify our task, since a simulation with nonzero quenched disorder needs averages over several disorder configurations, rendering the effort more time consuming than a clean-limit analysis. However, there is an important difference between the two cases: observing the resistivity peak in the clean limit requires a *fine tuning* of λ.

For a nonzero Δ, the range of couplings with a resistivity peak is much wider (see in Sec. II C for a more detailed discussion). Fine tuning is not compatible with the CMR effect since the phenomenon appears in a large number of manganese oxides, with a distribution of λ's. Nevertheless, while it is clear that working at nonzero Δ and smaller than critical λ is more realistic, to the extent that the emphasis of a clean-limit investigation in a fine-tuned range of λ is restricted to the vicinity of the Curie temperature, then both approaches appear to lead to similar conclusions.

Note that at very low temperatures the clean limit result shows insulating behavior, while the results with a nonzero disorder strength do not present such a feature. Although this fact establishes an interesting difference between the two cases, and in addition it is known that some manganites do present such an upturn in resistivity at low temperatures,[20] the issue will not be studied in detail in the rest of the manu-

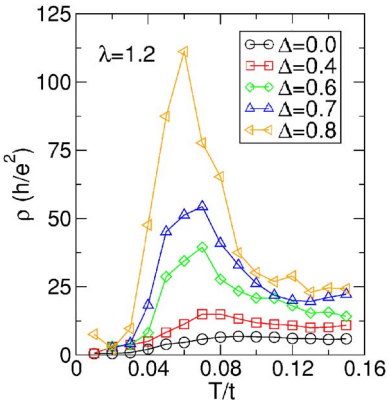

FIG. 3. (Color online) Influence of the disorder strength Δ (indicated) on the resistivity versus temperature curves, working at $\lambda=1.2$, $n=0.1$, and using an 8×8 lattice.

script since the focus of the effort is in the resistivity peak near the Curie temperature. The analysis of the puzzling low-temperature resistivity upturn in the clean limit is left for future work.

It is also remarkable that the numerical results for resistivity resemble qualitatively the experimental data in the presence of magnetic fields. A typical example is shown in Fig. 2(b), where external fields of a small value in units of t are used. It is fair to remark that in this section a linear scale is used for ρ while in most of the materials with truly CMR effects a logarithmic scale is needed, showing that the magnitude of the effect discussed here is substantially smaller. Also note that the fields used here are small when compared with the natural unit, i.e., the hopping amplitude, but in physical units such as teslas a field $H=0.1$ can be substantial. These quantitative differences could be related to the small size of the Monte Carlo systems used or, more likely, with the absence of a strongly insulating charge-ordered orbital-ordered antiferromagnetic state as the direct competitor of the FM metallic state.

C. Density $n=0.1$

Several of the effects discussed at the realistic density $n=0.3$ in the Sec. II B were found to be magnified by reducing the electronic density. The lattice to be shown is now two dimensional, to illustrate the similarity systematically found between results in two and three dimensions. In Fig. 3, the influence of the quenched disorder strength Δ on the resistivity plots is shown. As in Fig. 1, the case of a "small" λ is considered first, namely one where in the clean limit the resistivity does not present insulating behavior. As found for $n=0.3$, with increasing Δ a prominent peak is generated, which is located at the Curie temperature (conclusion based on the study of spin correlations, not shown). The ratio of the maximum and minimum resistivities is now 30–50 in the range of Δ analyzed here, considerably larger than at $n=0.3$.

As remarked for $n=0.3$, there appear to exist analogies between the processes of increasing Δ at "small" λ and increasing λ in the absence of quenched disorder. This relation is clear as well at $n=0.1$, and part of the evidence is shown in Fig. 4(a), which was obtained in the clean limit. In a narrow λ range, a prominent resistivity peak is found, as in Fig. 2(a). Note the use of a logarithmic scale for the resistivity, showing that the magnitude of the effect is truly colossal.

The effect of magnetic fields at $n=0.1$ is very pronounced [see Fig. 4(b)], once again resembling the magnitude of the CMR effect in real materials. The region in the vicinity of the resistivity peak is the most affected. The magnetoresistance ratios [Fig. 4(c)] are as large as those reported in the real Mn oxides with the largest CMR effects. The trade-off is that the effect occurs only in a small window of λ, but this range, as well as the magnetoresistance value, can be further enlarged by adding quenched disorder.

For the particular case $n=0.1$, it is interesting to remark the abruptness of the changes in the resistivity near the peak in Fig. 4(a) that resemble a first-order transition. The same occurs at the equivalent density $n=0.9$, as shown in Figs. 5(a)–5(c). There, the results of a longer Monte Carlo time simulation are presented and these numbers strongly suggest that indeed a first-order transition occurs. The evidence is the jump found in (a) the spin correlations and (b) the resistivity. Also, in (c) the MC time evolution for the energy is shown. This presents sudden events, that resemble tunneling between two clearly distinct states. Note that the temperature chosen is slightly biased toward the highest energy state,

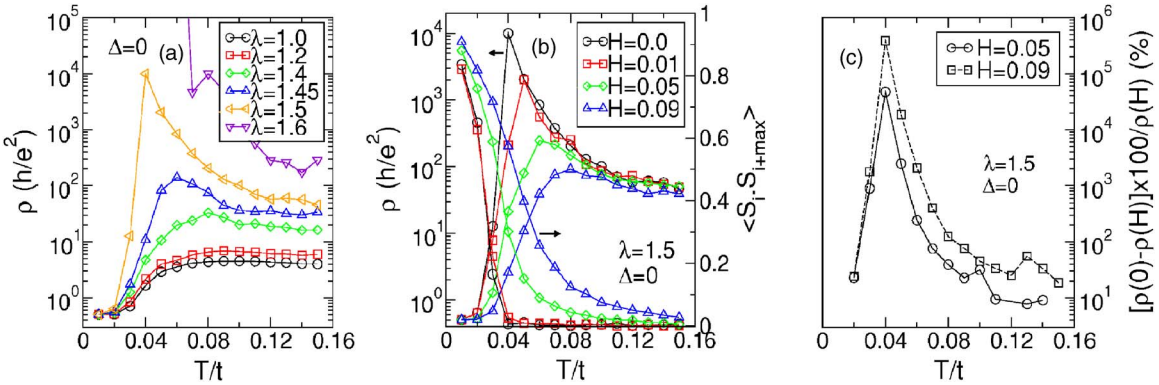

FIG. 4. (Color online) (a) Influence of the electron-phonon coupling λ on the resistivity versus temperature curves, (b) influence of magnetic fields on the resistivity curve and on the spin-spin correlation at the maximum allowed distance $(4\sqrt{2})$ on an 8×8 lattice, and (c) magnetoresistance ratios versus temperature, calculated for two representative magnetic fields in the clean limit $\Delta=0$, at $n=0.1$, and using an 8×8 lattice.

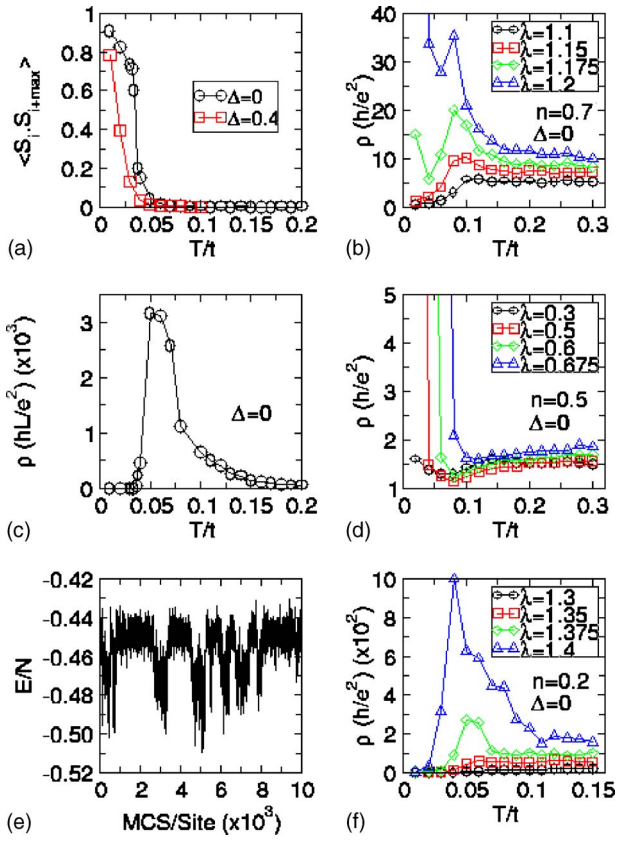

FIG. 5. (Color online). Results mainly in the clean limit $\Delta=0$ illustrating a variety of issues discussed in the text. (a),(b), and (c) The first-order (discontinuous) character of the transition at $n=0.9$, $\lambda=1.4$, using an 8×8 lattice. (a) The spin-spin correlations at the maximum distance. Also shown in red are results at $\Delta=0.4$ and averaged over five disorder configurations, showing the smearing of the transition with disorder; (b) is the resistivity versus T; and (c) is the Monte Carlo time evolution of the energy at $T=0.034$, showing the presence of two states. (d) The resistivity versus temperature at $n=0.7$ (8×8 lattice), at the λ's indicated. (e) The same as (d) but at $n=0.5$ and using a 12×12 cluster. (f) The same as (e) but for $n=0.2$.

since it is very difficult to fine tune T such that both competing states are visited an approximately equal amount of MC time. The first-order nature of the transition also highlights clear similarities with experiments for some manganites, such as $La_{0.7}Ca_{0.3}MnO_3$.

To finalize the study at density $n=0.1$, it is important to address to what extent quenched disorder (i.e., Δ) does play a key role in generating the resistivity peak. After all, both in this section and at $n=0.3$ it was observed that even in the clean limit $\Delta=0$ there is a λ range where a peak is present. The key observation is that while in the clean limit a *fine tuning* of λ is needed to obtain the resistivity peak, including quenched disorder the range becomes much wider. For instance, in Fig. 6(a) the area where a resistivity peak exists is shown in the λ-Δ plane. Avoiding fine tuning of couplings is crucial to understand CMR materials, since a wide variety of Mn oxides—with a distribution of bandwidths and couplings—present the CMR effects. Any proposed mechanism must be fairly universal to be robust, and the inclusion of quenched disorder indeed renders the range of couplings for CMR much wider than in the clean limit.

D. Other electronic densities and finite-size effects

The results presented thus far are only particular cases of the comprehensive analysis carried out in this effort, involving several electronic densities, couplings, and temperatures. As examples of other results obtained in the context of the one-orbital model, in Fig. 5(d) results at $n=0.7$ and in the clean limit are shown. A resistivity peak is also observed at $n=0.2$ for a 12×12 cluster [Fig. 5(f)], showing the robustness of the feature. However, the particular case $n=0.5$ is special since in this regime a staggered charge-ordered state is formed and, as a consequence, the system is strongly insulating at low temperatures in a wide range of electron-phonon couplings λ [see Fig. 5(e)]. This fact was also noticed in Ref. 36. Since at this density there is no peak in the resistivity, $n=0.5$ will not be further analyzed here.

To complete the present analysis, size effects have also

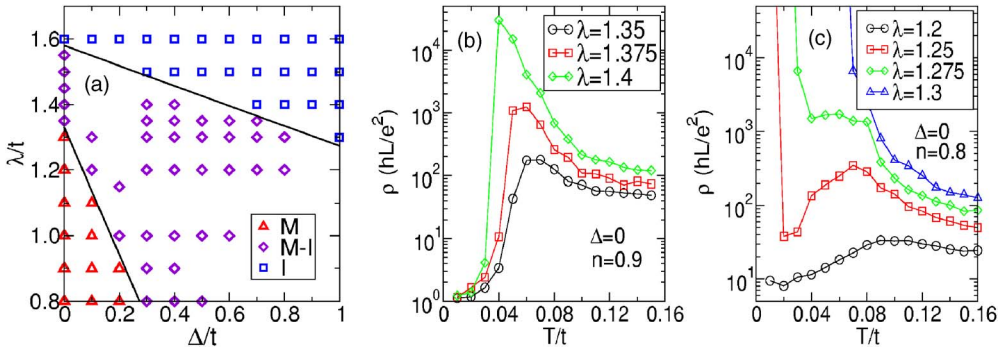

FIG. 6. (Color online) (a) Influence of quenched disorder on the size of the parameter-space region where the resistivity peak exists. In the plane λ-Δ, M (I) denotes the region where the resistivity is metallic (insulating) at all temperatures, while M-I is the area where the resistivity peak is present. The calculation was done on an 8×8 cluster, with $n=0.1$; (b) and (c) illustrate the similarity of results obtained using a $6\times6\times6$ lattice (shown) as compared with the $4\times4\times4$ results discussed before. (b) Resistivity versus temperature at $n=0.9$ in the clean limit $\Delta=0$, for the λ's indicated. (c) Resistivity ρ versus T at $n=0.8$ at the λ's indicated and for $\Delta=0$.

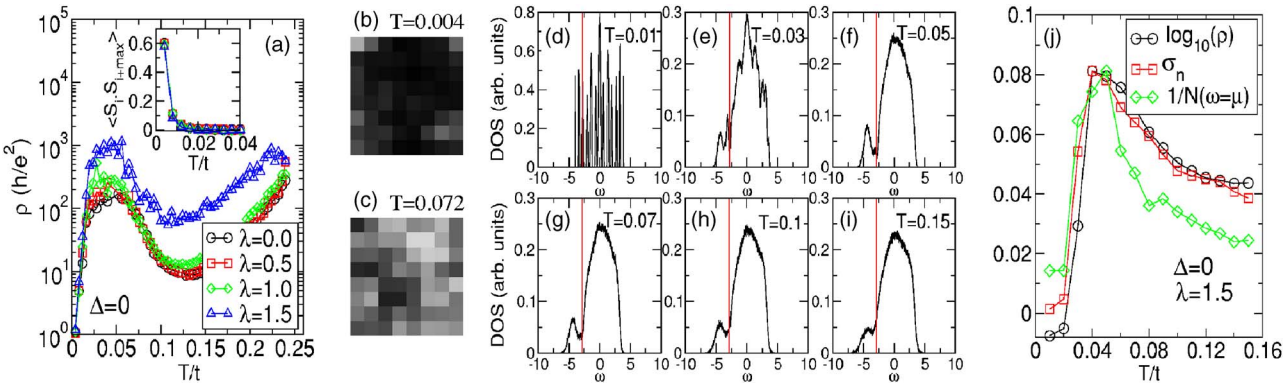

FIG. 7. (Color online) (a)–(c) Results obtained in the one electron limit. (a) Resistivity ρ versus T at $\Delta=0$ for an 8×8 lattice, showing that even the $\lambda=0$ results present a peak. The inset contains the spin-spin correlations at the maximum distance; (b), (c) the $\lambda=0$ spatially resolved nearest-neighbor spin-spin correlations $NN(i)=\Sigma_{\langle ij\rangle}\vec{S}_i\cdot\vec{S}_j$, where the sum is over the four neighbors j of site i. The results were obtained at $T=0.004$ and $T=0.072$, respectively, namely before and after the resistivity peak. Dark colors denote large values of $NN(i)$, namely regions where the spins are aligned ferromagnetically. (d)–(i) Density-of-states at $\lambda=1.5$, $\Delta=0$, using an 8×8 lattice, at the various temperatures indicated. The red lines (vertical) indicate the location of the chemical potential such that $n=0.1$ in all the panels. (j) Natural logarithm of the resistivity ρ versus temperature plotted on the same scale with σ_n (defined in text) and the inverse of the density of states at the chemical potential, $1/N(\omega=\mu)$, using the same parameters as in (d)–(i). Both $\log_{10}(\rho)$ and $1/N(\omega=\mu)$ are normalized to coincide with the maximum of σ_n. Results shown correspond to averages over several independent Monte Carlo runs.

been investigated. It was one of our purposes to use the standard "exact diagonalization" (ED) method in this study, in order to avoid considering also issues of accuracy if an approximate technique would have been employed, in addition to the intrinsic subtleties related with the physics involved in the problem. Moreover, we wanted to compare our results against those obtained with approximate methods carried out on $8\times8\times8$ lattices.[36] The penalization for using the ED method is that it is possible to carry out simulations only on up to $6\times6\times6$ clusters and compare those with the $4\times4\times4$ systems used in the figures discussed so far. The results are in Figs. 6(b) and 6(c). The existence of the resistivity peak, the overall shape of the curves, and the dependence with λ are very similar between the two lattices, supporting the conclusion that the results are robust and that indeed a CMR regime has been identified in these simulations (and in those reported before in Ref. 36).

E. The one-electron problem

The results reported in the previous sections indicate that the magnitude of the resistivity peak, namely the ratio between the maximum and minimum resistivities, increases when reducing the density n. In fact, the CMR effect is much larger at $n=0.1$ than at $n=0.3$. As a consequence, it is natural to wonder if for the case of just *one* electron a peak in the resistivity will also appear. Our effort is carried out in the grand canonical ensemble, but it is possible to tune the chemical potential with sufficient accuracy so that just one mobile electron is MC simulated. The results are shown in Figs. 7(a)–7(c), obtained on an 8×8 cluster. It is remarkable to find that indeed the one-electron problem has a resistivity versus temperature curve clearly resembling those of the other electronic densities. The inset of Fig. 7(a) shows that ferromagnetism in the classical spins is obtained in this case as well. In the bulk, likely only a finite-size FM region can be associated with a single electron, but on a finite small cluster this region can be as large as the entire system, as it occurs in our case.

An interesting detail of the one-electron study is that the insulating regime is observed even at $\lambda=0$. This occurs only at this very small electronic density; at $n=0.1$ or 0.3, a robust value of λ is needed to see a similar behavior. This can be understood as follows. The cluster spin-spin correlations are sketched in Fig. 7(b) at low temperature: here the entire 8×8 cluster is ferromagnetic in agreement with expectations. However, at higher temperatures, in the "insulating" portion of the $\lambda=0$ resistivity curve, there are patches that are FM as well, as shown in Fig. 7(c). This is correlated with charge localized in the darker regions (not shown).[45] Namely, in the insulating regime there is a "self-trapping" of the electrons that takes place, in the form of a small FM polaron. The lattice does not need to be distorted to see this curious effect. At temperatures higher than $T\sim0.125$, the resistivity now changes to a metallic state with a more uniform distribution of charge. The FM polarons at intermediate temperatures have sizes involving several lattice spacings and, thus, as n grows it is not surprising that their overlap rapidly renders the system fully metallic. At densities $n=0.1$ or larger, only with increasing λ is that a charge localized regime (with small polarons) can be achieved. This issue will be discussed in more detail in Sec. II F. Overall, the one electron case shows a resistivity profile similar to other densities, but the origin of the insulating state resides on the spin degree of freedom rather than the phononic, and in this respect it is anomalous.

F. Intuitive understanding of the results

To intuitively understand the results, the picture emerging from the one electron problem is important. It seems that upon cooling a paramagnetic metal first turns into an insula-

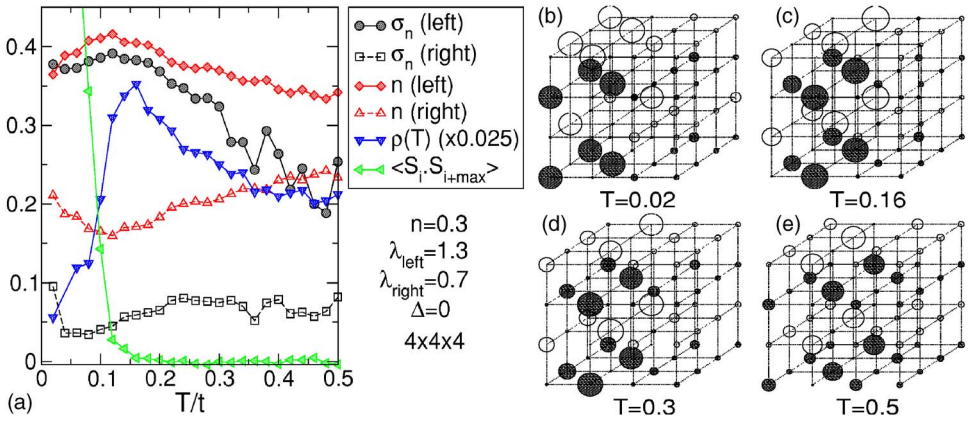

FIG. 8. (Color online) Possible explanation for the existence of the resistivity peak, using a $4\times4\times4$ and the couplings and densities indicated. Results shown are for the artificial "left-right" system described in the text, where the left (right) of the lattice has a relatively large (small) λ. (a) Various quantities (see middle inset) versus temperature. The growth of σ_n (left) and n (left) with decreasing temperature is indicative of localization of charge in the large λ region (left). The trends in these quantities are very similar to the resistivity in its insulating range. At the Curie temperature (see spin-spin correlations), the localization features remain the same but now the mobile carriers can conduct much better than in a paramagnetic spin background. (b)–(e) Electronic density (proportional to the diameter of the spheres) at the temperatures indicated.

tor via localization of charge (this is the insulating regime of the resistivity curve) and then, fairly abruptly, a transition to a metallic FM state occurs. Although we have not calculated the entropy explicitly (this is typically complicated to do in numerical simulations), we believe that in the range of λ's where this phenomenon occurs, there is a competition between a FM metallic state and a charge localized (CL) state. The former has lower energy, but the latter has higher entropy due to the fact that the charge can be localized in a variety of arrangements. For this reason at high temperature the CL state dominates, but then a crossing to the FM metal occurs at low temperatures.

This intuitive picture is compatible with a visual investigation carried out in this effort. In the interesting coupling and density regimes, Monte Carlo snapshots of the classical spin configurations and electronic density of charge systematically reveal charge localization in the insulating region. This is correlated with the appearance of new structure in the density-of-states (DOS), as shown in Figs. 7(d)–7(i). In this figure, the DOS is shown for the case $n=0.1$ varying the temperature in the interesting regime identified in Fig. 4. The DOS starts developing a pseudogap (PG) feature at the chemical potential at $T=0.15$. This PG grows upon cooling and it reaches its maximum depth at the temperature where the resistivity is maximized. Upon further cooling, the DOS turns into a typical FM density-of-states of a finite system, showing multiple spikes.[20] The presence of a PG in the DOS of a model for manganites was first observed in Ref. 8, and our present results are compatible with those early observations. Clearly, the resistivity peak is unrelated with Anderson localization that produces a mobility edge in the DOS, but not a PG.

The ideas discussed here related with DOS pseudogaps and charge localization can be made more quantitative as follows. In Fig. 7(j), the inverse of the DOS at the chemical potential is shown, together with the logarithm of the resistivity. Both quantities show a similar trend with temperature, and the PG indeed appears correlated with the behavior of the resistivity. However, note that the use of the logarithmic scale for ρ indicates that the effect leading to the PG formation affects much more strongly the transport properties of the system than others. This is typical of a percolative system where small changes in the electronic distribution can lead to dramatic changes in the transport characteristics.

For systems without quenched disorder the average local density is always constant due to translational invariance. Therefore, we measure the localization of the charge by calculating the error in n_i given by

$$\sigma_n^2 = \frac{1}{N}\sum_i |n_i - n|^2. \tag{3}$$

This quantity indicates the difference between the actual charge n_i at each site and the nominal average density in the full cluster, i.e., n. For a system with a uniform distribution of charge σ_n vanishes. This indeed occurs at very low temperatures. But for a system with charge localization then σ_n is different from zero, as it occurs at the resistivity peak. In Fig. 7(j), σ_n is plotted versus temperature, showing that it follows the behavior of the resistivity indicating that localization of the charge is the main reason for the insulating regime observed above the Curie temperature.

To gain further qualitative understanding for the existence of the peak in the resistivity, we have studied a special cluster that seems to have common features with those analyzed thus far. The cluster is a $4\times4\times4$ lattice, where the 32 sites on the right have a relatively small λ, i.e., not strong enough to lead to localization of charge, while the 32 sites on the left have a large λ. This allows us to clearly separate in space regions with and without charge localization. Monte Carlo simulating this system lead us to the resistivity and spin-spin correlations shown in Fig. 8(a). The shape is very similar to that of other simulations previously described. An important point to notice is that the total amount of charge on the left

side of the cluster grows with decreasing temperature and so does σ_n, the quantity that measures the degree of localization. The increase of these two quantities with cooling (shown in the figure as well) is correlated with the increase of resistivity, namely with the insulating regime in the resistivity plot. Thus, it is clear that the insulator portion of the resistance is caused by charge localization. Examples of the local densities are in Figs. 8(b)–8(e).

At the temperature where the resistivity turns metallic upon cooling, namely at the Curie temperature, note that the localization parameters remain approximately the same as at higher temperatures. Thus, the amount of charge that is localized does *not* change dramatically at the metal-insulator transition. What does change is the spin background and since the conducting properties of a ferromagnet and a paramagnet are very different, then there is a remarkable reduction of the resistance below the Curie temperature. The combination of these two effects leads to the resistivity peaks found in the Monte Carlo simulations.

III. TWO-ORBITAL MODEL

A. Definition

The two orbitals used in this model arise from the two e_g bands that are active at the Mn ions in Mn-oxides, as extensively discussed before.[10,20,23] The Hamiltonian for this model is[10,20,23]

$$H_{2b} = \sum_{\gamma,\gamma',i,\alpha} t^{\alpha}_{\gamma\gamma'} \mathcal{S}(\theta_i,\phi_i,\theta_{i+\alpha},\phi_{i+\alpha}) c^{\dagger}_{i,\gamma} c_{i+\alpha,\gamma'} + \lambda \sum_i (Q_{1i}\rho_i + Q_{2i}\tau_{xi} + Q_{3i}\tau_{zi}) + \sum_i \sum_{\alpha=1}^{\alpha=3} D_\alpha Q^2_{\alpha i}, \quad (4)$$

where the factor that renormalizes the hopping in the $J_H=\infty$ limit is

$$\mathcal{S}(\theta_i,\phi_i,\theta_j,\phi_j) = \cos\left(\frac{\theta_i}{2}\right)s\left(\frac{\theta_j}{2}\right) + \sin\left(\frac{\theta_i}{2}\right)\sin\left(\frac{\theta_j}{2}\right)e^{-i(\phi_i-\phi_j)}. \quad (5)$$

The parameters $t^{\alpha}_{\gamma\gamma'}$ are the hopping amplitudes between the orbitals γ and γ' in the direction α. In this section, we restrict ourselves to two dimensions, such that $t^x_{aa}=-\sqrt{3}t^x_{ab}=-\sqrt{3}t^x_{ba}=3t^x_{bb}=1$, and $t^y_{aa}=\sqrt{3}t^y_{ab}=\sqrt{3}t^y_{ba}=3t^y_{bb}=1$. Q_{1i}, Q_{2i}, and Q_{3i} are normal modes of vibration that can be expressed in terms of the oxygen coordinate $u_{i,\alpha}$ as

$$Q_{1i} = \frac{1}{\sqrt{3}}[(u_{i,z}-u_{i-z,z}) + (u_{i,x}-u_{i-x,x}) + (u_{i,y}-u_{i-y,y})],$$

$$Q_{2i} = \frac{1}{\sqrt{2}}(u_{i,x}-u_{i-x,x}),$$

$$Q_{3i} = \frac{2}{\sqrt{6}}(u_{i,z}-u_{i-z,z}) - \frac{1}{\sqrt{6}}(u_{i,x}-u_{i-x,x}) - \frac{1}{\sqrt{6}}(u_{i,y}-u_{i-y,y}).$$

Also, $\tau_{xi}=c^{\dagger}_{ia}c_{ib}+c^{\dagger}_{ib}c_{ia}$, $\tau_{zi}=c^{\dagger}_{ia}c_{ia}-c^{\dagger}_{ib}c_{ib}$, and $\rho_i=c^{\dagger}_{ia}c_{ia}+c^{\dagger}_{ib}c_{ib}$. The constant λ is the electron-phonon coupling related to the Jahn-Teller distortion of the MnO_6 octahedron.[2,8,10,11,14,20,22,23] Regarding the phononic stiffness, and in units of $t^x_{aa}=1$, the D_α parameters are $D_1=1$ and $D_2=D_3=0.5$, as discussed in previous literature.[46] The rest of the notation is standard. Note that in the large Hund coupling limit there is no spin index. The J_{AF} coupling between the localized spins is neglected, as for the one-orbital model. In some of the results below, a Zeeman term with field strength H was added. The number of Monte Carlo steps and MC starting configurations are similar to the one-band case.

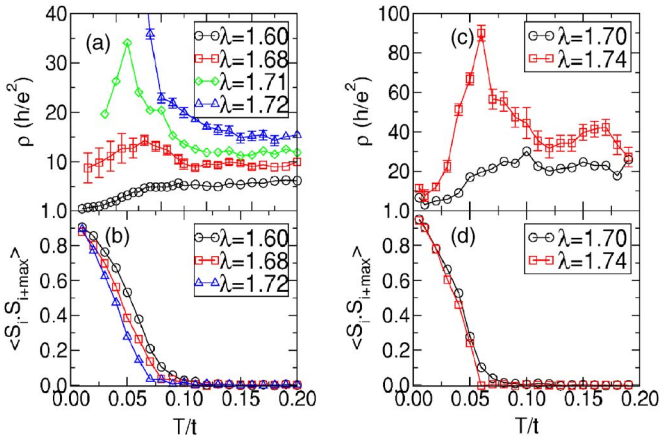

FIG. 9. (Color online) Clean limit ($\Delta=0$ results) (a): Resistivity versus T for various values of λ, using the two-orbital model for manganites. The simulation was performed on an 8×8 lattice with 20 electrons ($n\approx0.3$). (b) Spin-spin correlation at the maximum distance versus T for various values of λ. Lattice, density, and MC steps are as in (a). (c) Resistivity versus T for a 12×12 lattice, considering 2 orbitals per site, 44 electrons ($n\sim1/3$), $J_{AF}=0.0$, and the values of λ indicated. (d) Spin-spin correlation at the largest possible distance ($6\sqrt{2}$) on a 12×12 lattice, in the clean limit, with the same convention and parameters as in (a).

The main purpose of the numerical study discussed in this section is to investigate if the two-orbital model for manganites can also produce a resistivity peak, as observed in the one-orbital case. The study in this section is presented with the same caveats as the one-orbital investigation: (i) it is an important step toward a realistic theoretical description of manganites since Mn-oxides have two active e_g orbitals, but (ii) the model does not include the coupling J_{AF} which is crucial to generate the realistic insulating state, with antiferromagnetic and orbital order. Nevertheless, the observation of features that in several ways resemble experiments is exciting and at least part of the essence of real materials appears to have been captured by the models discussed here, even in purely FM regimes. We are aware that conclusions similar to ours have also been reached recently independently by Kampf and Kumar.[47]

B. Density $n=0.3$

Typical computational results for the two-orbital model at $n\sim0.3$ are shown in Fig. 9(a). In the clean limit $\Delta=0$, there is a narrow region of λ where a well-defined peak is found in the resistivity. The location of the peak is correlated with the

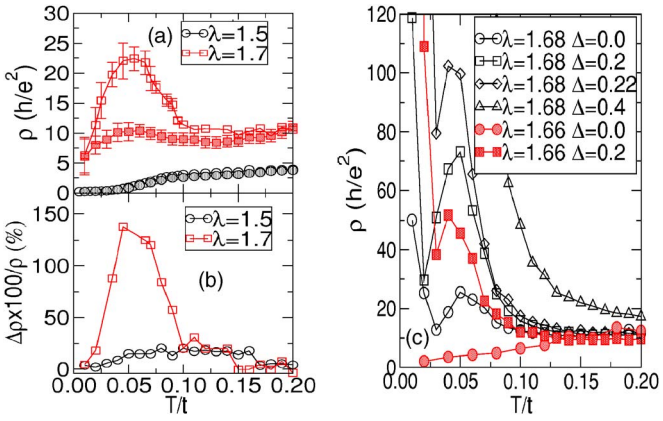

FIG. 10. (Color online) (a) Resistivity versus T for several λ's (indicated). Results were obtained with (closed symbols) and without (open symbols) a magnetic field $H=0.1$. The simulation was performed on an 8×8 lattice, with 20 electrons ($n\approx0.3$). (b) Magnetoresistance (defined as $((\rho(0)-\rho(H))/\rho(H))\times100$ versus T for the same parameters as in (a). (c) Resistivity versus T for various values of λ and with and without quenched disorder, as indicated. The enhancement of the resistivity peak with increasing Δ is shown. The lattice size and various parameters are as in Figs. 9(c) and 9(d).

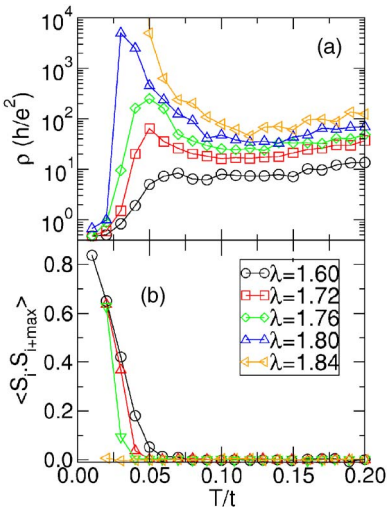

FIG. 11. (Color online) Results for the two-orbital model at $n=0.1$ and the λ's indicated. (a) Resistivity versus temperature using an 8×8 lattice. Note how sharp is the low temperature transition from low to high resistance. (b) Spin-spin correlation at the maximum distance.

appearance of ferromagnetic order, as shown in Fig. 9(b). The systematic tendencies and behaviors observed in the two-orbital model simulations are very similar to those found for the one-orbital model.

Finite-size effects do not seem to modify strongly our conclusions, as also found for the one-orbital case. In Fig. 9(c), results obtained using a 12×12 cluster are reported. A resistivity peak is observed in a very similar range of λ as found using the 8×8 cluster. Although these results are not sufficient to fully prove that the behavior found on finite lattice survives the bulk limit, they are very suggestive: in two- and three-dimensional lattices, for a wide range of electronic densities, for a variety of lattice sizes, with and without quenched disorder, and both for the one- and two-orbital models the resistivity peak is present in the study of charge transport.

This resistivity peak in the two-orbital model is also drastically affected by relatively small magnetic fields, as observed for the one-orbital case. Typical results are in Figs. 10(a) and 10(b). The magnitude of the magnetoresistance effect shown in the figure is comparable to the numbers found for the one-orbital case at similar electronic densities [see Fig. 2(c)].

It is also important to discuss the influence of quenched disorder. Typical results are in Fig. 10(c). As anticipated from recent previous investigations,[36] and from the one-orbital study in this manuscript, it was observed that introducing quenched disorder enhances substantially the features found in the clean limit. For instance, at $\lambda=1.66$, the $\Delta=0$ curve does not show a resistivity peak, but this feature is generated at $\Delta=0.2$ and the same λ. In cases where the resistivity already has a peak in the clean limit, this structure is enlarged with increasing Δ.

C. Density $n=0.1$

In Fig. 11, Monte Carlo results at $n=0.1$ are presented for the two-orbital model. The behavior of the resistivity is very similar to what was observed for the one-orbital case [see Figs. 6(b) and 4(b)], namely a clearly defined peak is observed, and a sharp (likely first order) transition in the resistance occurs upon cooling through the Curie temperature. At this electronic density, the changes in resistance upon heating or cooling are much larger than at other densities such as $n=0.3$.

Overall, it is clear that the models with one and two orbitals behave fairly similarly, and the existence of a peak in the resistivity is a robust result of this effort and previous Monte Carlo simulations.[36]

IV. CONCLUSIONS

The research effort discussed in this paper reached several goals. First, it confirmed recent reports by other groups[21,36] regarding the existence of a large peak in the resistivity versus temperature for the one-orbital model for manganites, including a robust electron-phonon coupling. This confirmation is interesting since the results of the previous[36] and current efforts were obtained using different techniques to estimate transport properties, and also with different methods to simulate the one-orbital model. Second, a comprehensive analysis of the influence of couplings, quenched disorder strength, and electronic density was here described. This includes the case of just one electron on an otherwise carrier empty lattice, in the presence of classical t_{2g} spins. This one-electron problem also presents a large resistance peak when varying the temperature. A very simple explanation for the behavior of these systems was discussed, based on a competition between tendencies to charge localization and ferromagnetism.

The work described here also includes a study of the two-orbital model for manganites. The overall conclusion is that its behavior is similar to that of the one-orbital model. Since these results are themselves also fairly similar to experi-

ments, our effort and those of other groups provide evidence that the theoretical studies based on double-exchange models that focus on the regime of competition between a metal and an insulator are on the right track toward a full explanation of the CMR phenomenon (for a different perspective see Ref. 42). Both with one and two orbitals, quenched disorder is important to enlarge the magnitude of the effects and broaden its range in parameter space, thus avoiding the fine tuning of couplings needed in the clean limit.

How do these results fit into the general picture advocated by some of the authors[10,20] in recent literature? In those early investigations, the competition between a metal and an insulator was the key new factor introduced to account for CMR. This competition is also present in the current effort, involving a FM metallic versus a FM insulating polaronic state. What is different is that in the present and related investigations[21,36] both the metal and the insulator at low temperatures are ferromagnetic, and they differ only in the arrangement of charge (extended versus localized character). We believe that this is the main reason for having obtained resistivity curves that while qualitatively resembling experiments, they still do not correspond to the huge magnetoresistance values observed in real CMR materials unless the densities are tuned to small values. The next level of sophistication of the simulations of manganite models must address the competition between different magnetic orders. Although the current results have a qualitative resemblance with several experiments, it is known that the largest effects in real manganites occur when an antiferromagnetic/charge/orbital ordered state competes with the ferromagnetic metal. To achieve this final goal, the coupling J_{AF} must be incorporated in the investigations. This will require levels of numerical accuracy higher than in the present effort, due to the competition of very different states that typically lead to metastabilities and long thermalization times. Results will be presented in the near future.

ACKNOWLEDGMENTS

We thank S. Kumar and A. Kampf for useful conversations. This work was supported in part by the LDRD program at ORNL and by the NSF Grant No. DMR-0443144. Most of the computational work in this effort was performed at the supercomputing facilities of the National Center for Computational Sciences at the Oak Ridge National Laboratory (ORNL), managed by UT-Battelle, LLC, for the U.S. Department of Energy under Contract No. DE-AC05-000R22725. We also acknowledge the help of J. A. Vergés in the study of conductances. This research used the SPF computer program and software toolkit developed at ORNL (http://mri-fre.ornl.gov/spf).

[1] Y. Tokura, *Colossal Magnetoresistive Oxides* (Gordon and Breach, New York, 2000).
[2] *Colossal Magnetoresistance, Charge Ordering, and Related Properties of Manganese Oxides*, edited by C. N. R. Rao and B. Raveau (World Scientific, Singapore, 1998).
[3] E. Dagotto, Science **309**, 258 (2005).
[4] A. Moreo, S. Yunoki, and E. Dagotto, Science **283**, 2034 (1999).
[5] M. R. Ibarra and J. M. D. Teresa, Mater. Sci. Forum **302-303**, 125 (1999).
[6] J. M. D. Teresa, M. R. Ibarra, P. A. Algarabel, C. Ritter, C. Marquina, J. Blasco, J. García, A. del Moral, and Z. Arnold, Nature (London) **386**, 256 (1997).
[7] J. W. Lynn, R. W. Erwin, J. A. Borchers, Q. Huang, A. Santoro, J. L. Peng, and Z. Y. Li, Phys. Rev. Lett. **76**, 4046 (1996).
[8] A. Moreo, S. Yunoki, and E. Dagotto, Phys. Rev. Lett. **83**, 2773 (1999).
[9] M. Uehara, S. Mori, C. H. Chen, and S.-W. Cheong, Nature (London) **399**, 560 (1999).
[10] E. Dagotto, T. Hotta, and A. Moreo, Phys. Rep. **344**, 1 (2001).
[11] M. B. Salamon and M. Jaime, Rev. Mod. Phys. **73**, 583 (2001).
[12] F. Parisi, P. Levy, L. Ghivelder, G. Polla, and D. Vega, Phys. Rev. B **63**, 144419 (2001).
[13] D. Louca, T. Egami, E. L. Brosha, H. Roder, and A. R. Bishop, Phys. Rev. B **56**, R8475 (1997).
[14] N. Mathur and P. B. Littlewood, Phys. Today **56** (1), 25 (2003).
[15] S. Yunoki, J. Hu, A. L. Malvezzi, A. Moreo, N. Furukawa, and E. Dagotto, Phys. Rev. Lett. **80**, 845 (1998).
[16] S. Yunoki and A. Moreo, Phys. Rev. B **58**, 6403 (1998).
[17] A. J. Millis, P. B. Littlewood, and B. I. Shraiman, Phys. Rev. Lett. **74**, 5144 (1995).
[18] A. J. Millis, B. I. Shraiman, and R. Mueller, Phys. Rev. Lett. **77**, 175 (1996).
[19] D. Khomskii and K. Kugel, Europhys. Lett. **55**, 208 (2001).
[20] E. Dagotto, *Nanoscale Phase Separation and Colossal Magnetoresistance* (Springer, Berlin, 2002).
[21] J. A. Vergés, V. Martín-Mayor, and L. Brey, Phys. Rev. Lett. **88**, 136401 (2002).
[22] K. H. Ahn, T. Lookman, and A. R. Bishop, Nature (London) **428**, 401 (2004).
[23] E. Dagotto, New J. Phys. **7**, 67 (2005).
[24] T. Hotta, A. L. Malvezzi, and E. Dagotto, Phys. Rev. B **62**, 9432 (2000).
[25] Y. Motome, N. Furukawa, and N. Nagaosa, Phys. Rev. Lett. **91**, 167204 (2003).
[26] Y. Motome and N. Furukawa, J. Phys. Soc. Jpn. **69**, 3785 (2000), **70**, 3186 (2001).
[27] Y. Motome and N. Furukawa, J. Phys. Soc. Jpn. **68**, 3853 (1999).
[28] R. Mathieu, D. Akahoshi, A. Asamitsu, Y. Tomioka, and Y. Tokura, Phys. Rev. Lett. **93**, 227202 (2004).
[29] J. Salafranca and L. Brey, cond-mat/0602392.
[30] M. J. Calderón, J. A. Vergés, and L. Brey, Phys. Rev. B **59**, 4170 (1999).
[31] E. Nagaev, JETP Lett. **6**, 18 (1967).
[32] D. P. Arovas and F. Guinea, Phys. Rev. B **58**, 9150 (1998).
[33] M. Mayr, G. Alvarez, and E. Dagotto, Phys. Rev. B **65**, 241202(R) (2002).
[34] J. Burgy, M. Mayr, V. Martin-Mayor, A. Moreo, and E. Dagotto, Phys. Rev. Lett. **87**, 277202 (2001).

[35] J. Burgy, A. Moreo, and E. Dagotto, Phys. Rev. Lett. **92**, 097202 (2004).
[36] S. Kumar and P. Majumdar, Phys. Rev. Lett. **96**, 016602 (2006).
[37] S. Kumar and P. Majumdar, Phys. Rev. Lett. **94**, 136601 (2005).
[38] D. Akahoshi, M. Uchida, Y. Tomioka, T. Arima, Y. Matsui, and Y. Tokura, Phys. Rev. Lett. **90**, 177203 (2003).
[39] T. Nakajima, H. Kageyama, and Y. Ueda, J. Phys. Chem. **63**, 913 (2002).
[40] S. Kumar and P. Majumdar, Phys. Rev. Lett. **92**, 126602 (2004).
[41] T. Hotta, Y. Takada, H. Koizumi, and E. Dagotto, Phys. Rev. Lett. **84**, 2477 (2000).
[42] A. S. Alexandrov, A. M. Bratkovsky, and V. V. Kabanov, Phys. Rev. Lett. **96**, 117003 (2006).
[43] Note that in two dimensions the existence of metallicity is very subtle, involving Anderson localization effects. In our results, the sign of the resistivity versus temperature curves is our definition of metal or insulator, and it may occur that at very low temperatures or very large lattices localization effects may render the metal insulating in 2D. This difficult issue is beyond the scope of our current effort.
[44] J. A. Vergés, Comput. Phys. Commun. **118**, 71 (1999).
[45] Actually, for systems without quenched disorder the average local charge density is always constant. We later formalize the discussion presented here by introducing the quantity σ_n.
[46] H. Aliaga, D. Magnoux, A. Moreo, D. Poilblanc, S. Yunoki, and E. Dagotto, Phys. Rev. B **68**, 104405 (2003).
[47] A. Kampf and S. Kumar, poster presentation given at the workshop "Nanoscale Fluctuations in Magnetic and Superconducting Systems," Dresden, May, 2005.